RNA (1996), 2:244–253. Cambridge University Press. Printed in the USA.

Structure of 4.5S RNA in the signal recognition particle of *Escherichia coli* as studied by enzymatic and chemical probing

GEORG LENTZEN,[1] HERVÉ MOINE,[2] CHANTAL EHRESMANN,[2] BERNARD EHRESMANN,[2] and WOLFGANG WINTERMEYER[1]

[1] Institut für Molekularbiologie, Universität Witten/Herdecke, D-58448 Witten, Germany
[2] UPR No. 9002 du CNRS, Institut de Biologie Moléculaire et Cellulaire, 15 rue René Descartes, 67084 Strasbourg Cedex, France

ABSTRACT

The structure of 4.5S RNA, the *Escherichia coli* homologue of the signal recognition particle (SRP) RNA, alone and in the SRP complex with protein P48 (Ffh) was probed both enzymatically and chemically. The molecule is largely resistant against single strand-specific nucleases, indicating a highly base paired structure. Reactivity appears mainly in the apical tetraloop and in one of the conserved internal loops. Although some residues are found reactive toward dimethylsulphate and kethoxal in regions predicted to be unpaired by the phylogenetic secondary structure model of 4.5S RNA, generally the reactivity is low, and some residues in internal loops are not reactive at all. RNase V1 cleaves the RNA at multiple sites that coincide with predicted helices, although the cleavages show a pronounced asymmetry. The binding of protein P48 to 4.5S RNA results in a protection of residues in the apical part of the molecule homologous to eukaryotic SRP RNA (domain IV), whereas the cleavages in the conserved apical tetraloop are not protected. Hydroxyl radical treatment reveals an asymmetric pattern of backbone reactivity; in particular, the region encompassing nucleotides 60–82, i.e., the 3′ part of the conserved domain IV, is protected. The data suggest that a bend in the domain IV region, most likely at the central asymmetric internal loop, is an important element of the tertiary structure of 4.5S RNA. Hyperchromicity and lead cleavage data are consistent with the model as they reveal the unfolding of a higher-order structure between 30 and 40 °C. Protection by protein P48 occurs in this region of the RNA and, more strongly, in the 5′ part of domain IV (nt 26–50, most strongly from 35 to 49). It is likely that P48 binds to the outside of the bent form of 4.5S RNA.

Keywords: hydroxyl radical probing; lead-catalyzed cleavage; protein translocation; ribonucleoprotein; 7S RNA; SRP; SRP54

INTRODUCTION

Signal recognition particle (SRP) functions as an adaptor between the translating ribosome and the membrane of the endoplasmic reticulum (ER) (reviewed in Walter & Johnson, 1994; Lütcke, 1995). SRP recognizes ribosomes exposing a signal sequence (Walter et al., 1981; Siegel & Walter, 1988) and targets them to the SRP receptor anchored in the ER membrane (Gilmore et al., 1982; Meyer et al., 1982). From there, the nascent chain–ribosome complex is delivered to the translocation site in the ER membrane in a GTP-dependent process (Connolly & Gilmore, 1989). Mammalian SRP, which has been characterized most extensively, consists of SRP RNA (300 nt) and six polypeptides (SRP9, 14, 19, 54, 68, 72) (Walter & Blobel, 1982). Homologues of SRP RNA have been found in many eucaryotes, archaea, and bacteria (Larsen & Zwieb, 1990; Zwieb & Larsen, 1994). Phylogenetic comparisons indicate that the SRP RNA folds into a conserved structure (Poritz et al., 1988; Larsen & Zwieb, 1990; Althoff et al., 1994). The structure can be divided into four domains (Poritz et al., 1988), of which domain IV shows the highest conservation of both sequence and secondary structure. The SRP RNA homologue in *Escherichia coli*, 4.5S RNA (114 nt), also contains a hairpin structure homologous to domain IV, but lacks domain I, III, and most of domain II present in the mammalian and archaebacterial counterparts.

4.5S RNA forms a ribonucleoprotein complex with the P48 (Ffh) protein (Poritz et al., 1990; Ribes et al.,

Reprint requests to: Wolfgang Wintermeyer, Institut für Molekularbiologie, Universität Witten/Herdecke, D-58448 Witten, Germany; e-mail: glentzen@umi-wh.de.

1990), the *E. coli* homologue of the SRP54 protein of mammalian SRP (Bernstein et al., 1989; Römisch et al., 1989). In a mutagenesis study, several conserved residues in the internal loops of domain IV have been shown to be important for the binding of P48 (Wood et al., 1992). A complex homologous to the P48·4.5S RNA ribonucleoprotein has been found in *Mycoplasma mycoides*, and the protein was shown to protect the conserved domain IV region from RNase A cleavage (Samuelsson, 1992). Genetic and biochemical evidence suggests that there is also functional homology to mammalian SRP (Luirink et al., 1992, 1994; Phillips & Silhavy, 1992; Bernstein et al., 1993; Miller et al., 1994). The *E. coli* ribonucleoprotein P48·4.5S RNA is able to bind the signal sequences of nascent presecretory proteins (Luirink et al., 1992) and forms a stable complex with the *E. coli* SRP-receptor FtsY in the presence of a nonhydrolyzable GTP analogue (Miller et al., 1994; Kusters et al., 1995). Furthermore, a complex of eukaryotic SRP54 and 4.5S RNA has been shown recently to promote translocation of nascent proteins (Hauser et al., 1995). Although the role of this essential RNA is still not understood, it is needed for the interaction of SRP with the SRP receptor FtsY (Miller et al., 1994) and has also been proposed to interact with the ribosome in the elongation cycle of protein synthesis (Brown, 1989).

Predictions of the 4.5S RNA secondary structure based on either thermodynamic parameters or phylogenetic comparison (Poritz et al., 1988; Larsen & Zwieb, 1990) point to a highly base paired rod-like structure (Fig. 2). In this model, the domain homologous to domain IV reaches from the apical tetraloop to the internal loop C and shows sequence conservation, especially in the internal loops. The distal part of the molecule reaching from helix d to the terminal GC-clamp is homologous to a part of domain II of mammalian SRP RNA (Larsen & Zwieb, 1990; Althoff et al., 1994), but does not contain strongly conserved nucleotides.

In a previous study, indications for a higher-order folding of the tertiary structure of 4.5S RNA that changes upon binding of protein P48 have been obtained (Lentzen et al., 1994). Here, we studied the structure of 4.5S RNA in detail by investigating the reactivity toward enzymatic and chemical probes. The effect of binding of protein P48 on the structure of the RNA was also tested and provides information about the P48 binding site on 4.5S RNA. The reactivity toward Fe(II)-EDTA and the Pb^{2+}-cleavage pattern reveal a tertiary structure folding in the conserved part of 4.5S RNA.

RESULTS

RNase cleavage of 4.5S RNA and of the complex P48·4.5S RNA

Enzymatic probing was performed with the single strand-specific RNases T1 and T2 and with RNase V1 that preferentially cleaves double-stranded or otherwise structured regions. The results obtained by primer extension with reverse transcriptase are shown in Figure 1; the summary of the results of enzymatic probing is given in Figure 2.

As a general rule, it is noted that the reactivity toward the single strand-specific RNases of residues in predicted internal loops is low, indicating a rather compact structure of the molecule with only a few accessible single-stranded positions. Major cuts by RNase T1 are located at G53 and G54 in the tetraloop, whereas

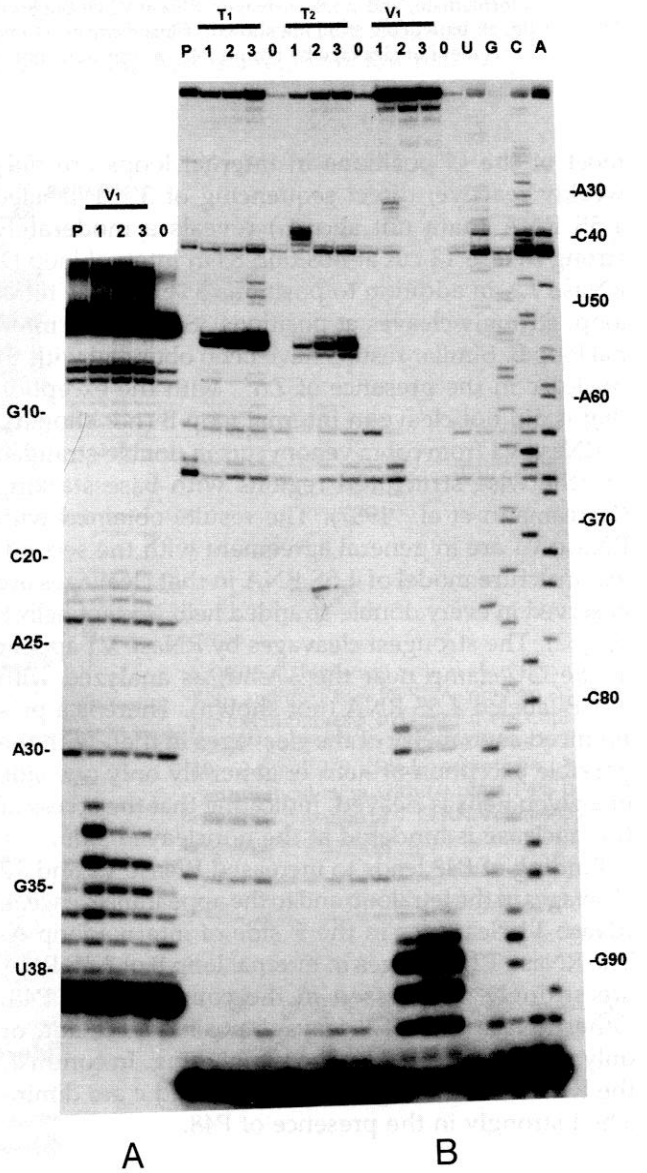

FIGURE 1. RNase cleavages of 4.5S RNA and the P48·4.5S RNA complex. **A:** RNase V1, primer complementary to nt 39–52. **B:** RNases T1, T2, V1, primer complementary to nt 94–105. Lanes 1, 4.5S RNA (10 pmol); lanes 2, 10 pmol P48 added; lanes 3, 20 pmol P48 added; lanes 0, control incubation of 4.5S RNA alone, lanes P, control incubation with P48; U, G, C, A, sequencing lanes. Cleavage reactions and sequencing by primer extension with reverse transcriptase are described in the Materials and methods.

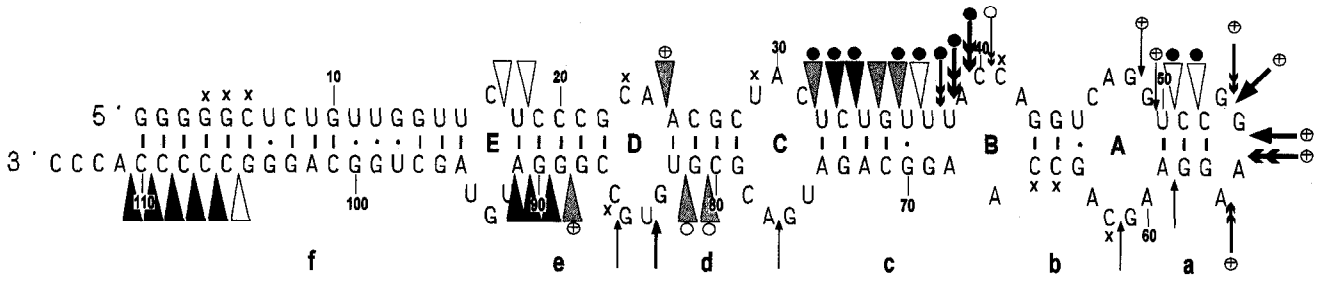

FIGURE 2. Patterns of cleavages of 4.5S RNA with RNases T1, T2, and V1. 4.5S RNA is depicted in the 2D structural model (Poritz et al., 1988) with labeling of internal loops and helices with capital and small letters, respectively, starting from the apical tetraloop. Distinct from other secondary structure models, helix c is shortened and does not include base pairs U37–G69 and U38–A68 (see text). RNase T1 cleavages (strong, intermediate, weak) are indicated by arrows of corresponding thickness; RNase T2 cleavages by double arrows; RNase V1 cleavages by arrowheads (black, gray, white for strong, intermediate, and weak cleavage). RNase V1 cleavages near the 3′ end were obtained with 3′-^{32}P-labeled 4.5S RNA and direct sequencing (data not shown). Closed circles, strong protection by P48; open circles, weak protection by P48; ⊕, enhancement of cleavage by bound P48; x, positions not included in the analysis due to pausing of reverse transcriptase.

most of the G positions in internal loops are only weakly reactive; direct sequencing of 3′-^{32}P-labeled 4.5S RNA (data not shown) reveals a moderately strong RNase T1 cut at position 83 in internal loop D. RNase T2, in addition to positions 53–55 in the tetraloop, strongly cleaves at positions 38 and 39 in internal loop B. Similar results have been obtained with S1 nuclease in the presence of Zn^{2+} with the exception that it did not cleave in internal loop B (not shown).

RNase V1 from cobra venom cuts in double-stranded or otherwise structured regions with base stacking (Ehresmann et al., 1987). The results obtained with RNase V1 are in general agreement with the secondary structure model of 4.5S RNA in that cleavages are observed in every double-stranded helix, except helix b (Fig. 2). The strongest cleavages by RNase V1 appear at the GC-clamp near the 3′ end, as analyzed with 3′-^{32}P-labeled 4.5S RNA (not shown). There is a pronounced asymmetry of the cleavages in that, with the possible exception of helix e, generally only one side of a given helix is cleaved, indicating that the access of the nuclease is hindered at the noncleaved side.

Binding of P48 leads to increased RNase T1 and T2 cleavages in the tetraloop and to the appearance of weak RNase T1 cleavages in the 5′ side of internal loop A. The RNase T2 cleavages in internal loop B of 4.5S RNA are strongly suppressed in the complex with P48. Other RNase T1 or T2 cleavage positions are not, or only slightly, affected by protein binding. In contrast, the RNase V1 cleavages in helices a and c are diminished strongly in the presence of P48.

Chemical probing of bases

A number of chemical reagents was used for probing the accessibility of specific nitrogen positions of bases (Ehresmann et al., 1987): DMS (N1 of adenine, N3 of cytidine), kethoxal (N1 and N2 of guanine), and CMCT (N3 of uracil, N1 of guanine) were used to map unpaired residues. DEPC reacts with a nitrogen not involved in normal base pairing (N7 of adenine), but adenines in double helices are unreactive (Ehresmann et al., 1987). Modification of these positions inhibits reverse transcriptase and can, therefore, be analyzed by primer extension.

The general result of the chemical probing is that 4.5S RNA is highly resistant against modification. At standard conditions, only residues A47 and C78 in the internal loops A and C, respectively, are reactive toward DMS, and kethoxal modifies only guanines in the tetraloop and at position G83 (not shown). A47, which is strongly protected by P48, was shown to be essential for P48 binding and cell viability (Wood et al., 1992). At higher concentration of DMS (5% (v/v)), adenines 30 and 77 in loop C, as well as 67 and 68 in loop B, are also modified strongly, whereas intermediate reactivity is observed at residues in the tetraloop and in loops A–D (data not shown; results summarized in Fig. 3). 4.5S RNA proved unreactive even at rather high concentrations of CMCT (4.2 mg/mL) and DEPC (12,5% (v/v)), indicating that the uracil residues in the internal loops of the secondary structure model are involved in some interactions and that the N7 positions of adenines are protected by base stacking or are involved in tertiary interactions.

The formation of the P48·4.5S RNA complex decreases greatly the reactivity against DMS of the strongly reactive adenines 47 (internal loop A) and 68. The reactivity of the bases in the tetraloop and in loops A–D is moderately or slightly reduced by P48 binding (Fig. 3).

Hydroxyl radical probing of the backbone

H_2O_2 in the presence of Fe(II)-EDTA leads to the formation of a reactive species, presumably a hydroxyl radical (Tullius, 1987), which cleaves the backbone of

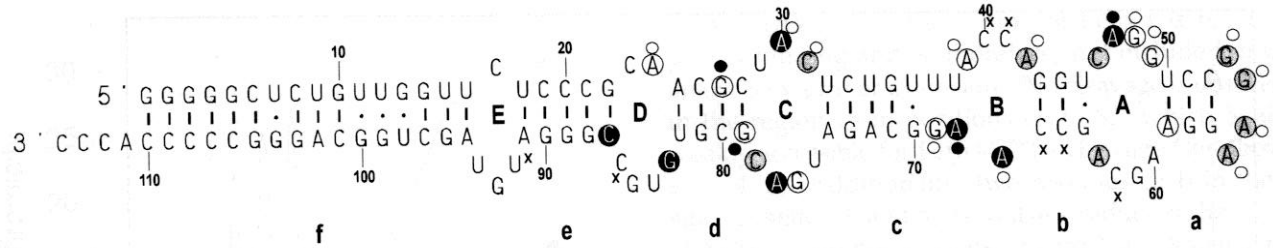

FIGURE 3. Modification of 4.5S RNA with DMS and kethoxal. The nucleotides are encircled according to their reactivity: ●, strong, ⊛, intermediate, and ○, weak; small circles above nucleotides indicate strong (●) and weak (○) protection by P48. x, positions not included in the analysis due to pausing of reverse transcriptase.

nucleic acids by reacting with C1′ and C4′ of (deoxy)ribose (Wu et al., 1983). The probe is insensitive to secondary structure and, therefore, valuable for probing the tertiary structure of RNAs (Latham & Cech, 1989).

The hydroxyl radical pattern obtained with free 4.5S RNA is highly asymmetric (Fig. 4, lanes 1). As shown by the quantitative analysis (Fig. 5A) and summarized in Figure 5B, there is a region of low reactivity, relative

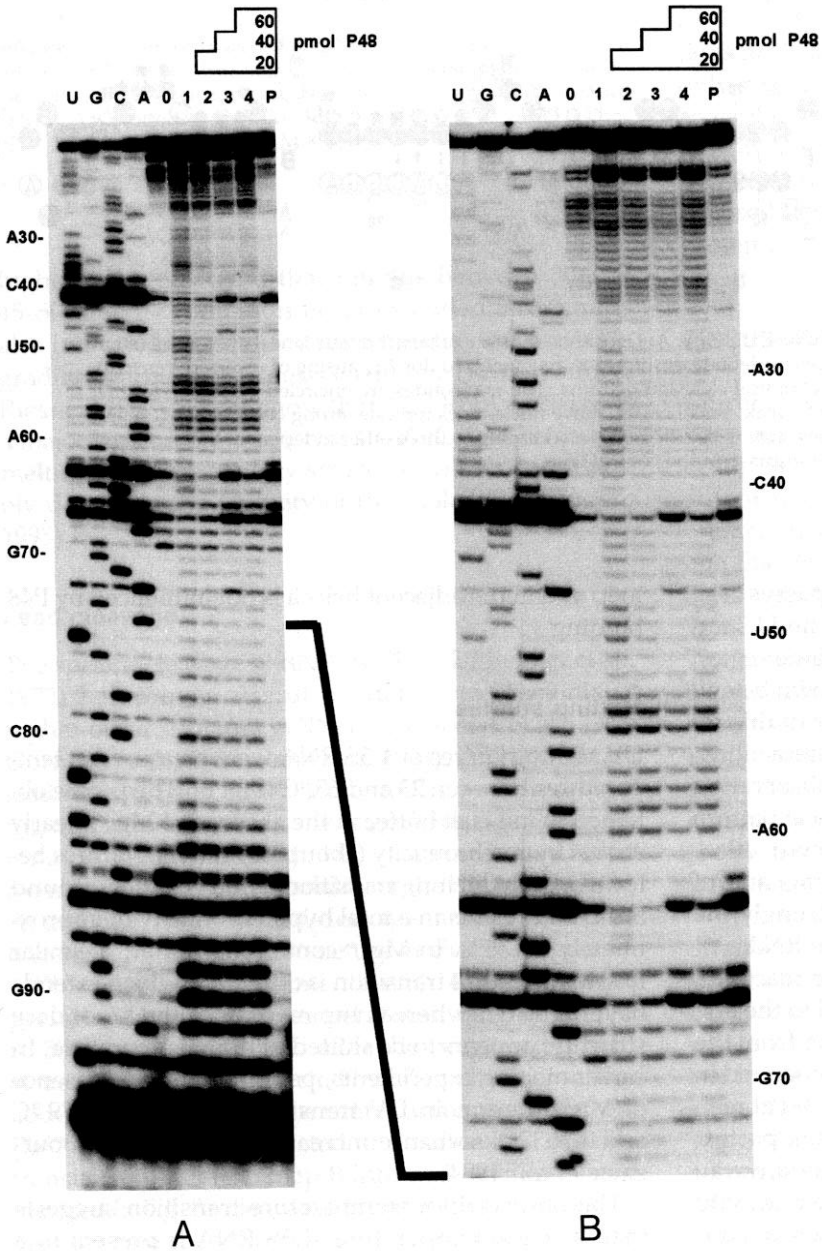

FIGURE 4. Hydroxyl radical cleavages of 4.5S RNA and the P48·4.5S RNA complex. **A:** Short-run electrophoresis. **B:** Long-run electrophoresis. Lanes 1, 4.5S RNA (20 pmol); lanes 2, 3, 4: 20, 40, 60 pmol P48 added, respectively; lanes P, control incubation with 60 pmol P48; lanes 0, control incubation of 4.5S RNA alone; U, G, C, A, sequencing lanes.

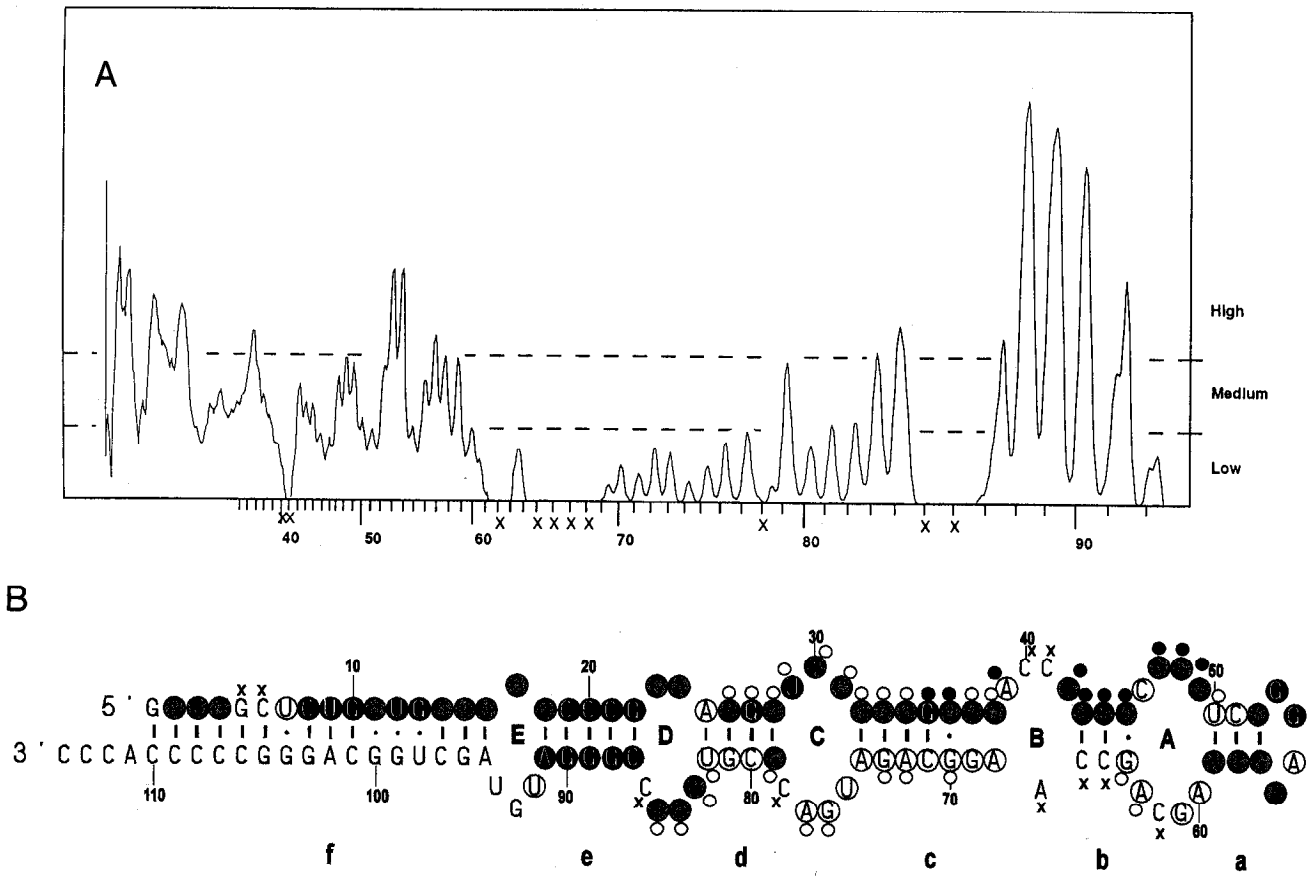

FIGURE 5. Hydroxyl radical cleavage pattern of 4.5S RNA. **A:** Densitometer trace of lane 1 minus lane 0 of Figure 4 (short run); ordinate in arbitrary units, abscissa gives nucleotide positions; x, not analyzed due to pausing of reversed transcriptase in the control. **B:** Summary of hydroxyl radical cleavage patterns. The nucleotides are encircled according to their reactivity: ●, strong, ◍, intermediate, and ○, weak. Small circles above nucleotides indicate strong (●) or weak (○) protection by P48. In B, the reactivity at positions A68, G85, C87 is given according to three other independent experiments where there was no pausing of reverse transcriptase in the control lane.

to other parts of the molecule, that encompasses residues 60–82, i.e., the 3′ sides of loops A, B, and C and of helices b, c, and d. It is noted that the same region is also not accessible to nucleases and, as shown below, to lead cleavage. The relative inaccessibility of this region indicates its involvement in tertiary interactions. In keeping with this interpretation is the observation of a more regular, symmetric hydroxyl radical pattern at higher temperature (40 °C; data not shown). Also, the results of hyperchromicity measurements and of lead cleavage, presented below, suggest strongly the existence of a higher-order structure of the RNA.

The effect of P48 binding in reducing the reactivity toward hydroxyl radicals is clearly restricted to the apical half of the 4.5S RNA molecule extending from the tetraloop into loop D (Fig. 4, lanes 2–4; summarized in Fig. 5). The strongest protections are observed at residues 35–49 in the 5′ side of this region, weak protections at residues 26–34, as well as at some, anyway weakly reactive, residues in the 3′ side. The reactivity toward hydroxyl radicals of the residues in the tetraloop and in the adjacent helix a is not influenced by P48 binding.

Melting studies

UV melting curves of 4.5S RNA were measured at temperatures between 23 and 65 °C (Fig. 6). The profile obtained in low-salt buffer in the absence of Mg^{2+} clearly shows hyperchromicity (about 8%) at temperatures below the main melting transition, which has a T_m around 50 °C and results in a total hyperchromicity of approximately 30–35%. In Mg^{2+}-containing buffer, a similar low-temperature transition is observed, which extends beyond 60 °C, whereas the melting of the secondary structure appears to be shifted to high temperature. In earlier melting experiments, performed in the presence of Mg^{2+}, one main UV transition with a T_m at 79 °C and a 35% absorbance increase was observed (Bourgaize et al., 1984).

The observed low-temperature transition suggests that, at room temperature, 4.5S RNA is present in a

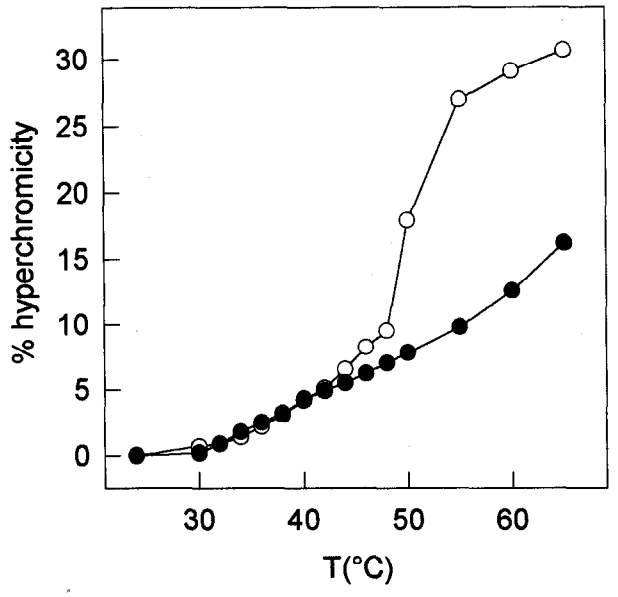

FIGURE 6. Melting curves of 4.5S RNA. Absorbance at 260 nm of a solution of 4.5S RNA was measured at various temperatures, as indicated. Absorbance increase relative to the initial absorbance (0.8 A_{260}) is plotted. ○, 20 mM HEPES, pH 7.5; ●, 20 mM HEPES, pH 7.5, 10 mM $MgCl_2$, 100 mM KCl.

higher-order structure that unfolds between 30 and 45–50 °C. The formation of an extended structure is also indicated by experiments using the temperature-gradient gel electrophoresis technique (Rosenbaum & Riesner, 1987). These show that 4.5S RNA undergoes a major structural transition at 40–45 °C, i.e., before the melting of the secondary structure, which considerably decreases the mobility of the molecule (Lentzen, 1995).

Lead cleavage

The specific cleavage of RNA by Pb^{2+} (Dirheimer et al., 1972) has proven useful for detecting elements of higher-order structure in RNA (Krzyzosiak et al., 1988; Gornicki et al., 1989; Pan et al., 1991). A predominant lead cleavage site either is due to the preferred binding of a lead ion to this site, signifying a binding site for a divalent cation, e.g., Mg^{2+}, or else it may reflect a particular structural flexibility of the RNA at this site. At any rate, a strong lead cleavage indicates the presence of a higher-order structure at the cleavage site.

Pb^{2+} cleavage experiments with 4.5S RNA were performed at different temperatures, ranging from 25 to 50 °C, i.e., before and after the presumed tertiary structure transition detected by UV melting described above. At the lower temperature, two extremely strong Pb^{2+} cleavages are detected at positions 37/38 at the transition of internal loop B into helix c (Fig. 7; summarized in Fig. 8); cleavages at other sites are weak, except for two moderately strong sites in the 5′ side of helix f. (As above, the 3′ side of helix f is used for primer binding and is, therefore, not included in the analysis by primer extension.) No cleavage is observed in the region from positions 69 to 82, which is also weakly accessible for Fe(II)-EDTA cleavage (see above, Figs. 4, 5). Additionally, two residues each in the 5′ sides of helices b and d, as well as residues at the 3′ side of helix d, are not reactive toward lead. Raising the temperature results in the complete disappearance of the preferential Pb^{2+}-catalyzed cleavage at positions 37/38 and leads to a more or less uniform pattern where cleavage occurs randomly at essentially all positions, including the ones that were not cleaved at the lower temperature (Fig. 7).

The influence of P48 binding on the lead cleavage of 4.5S RNA was studied at 25 °C (Fig. 7; summarized in Fig. 8). Enhancement of reactivity appears at G54 in the tetraloop. The most prominent effect is the strong protection of the predominant Pb^{2+} cleavage site at positions 37/38 of 4.5S RNA. It is noted that this is also the only region (except for the tetraloop) that is highly accessible for single strand-specific nucleases. The protection of this region, also against Pb^{2+}- and Fe(II)-EDTA cleavage, argues for an important role of this exposed tertiary structure element in the binding of P48 protein.

DISCUSSION

Current secondary structure models of 4.5S RNA have been derived from phylogenetic comparisons (Poritz et al., 1988; Larsen & Zwieb, 1990) and are largely consistent with the thermodynamically most stable secondary structure predicted by the algorithm of Zuker and Stiegler (1981). The predicted double-stranded helices, with the exception of the short helix b, are confirmed by the present data obtained with RNase V1. The accessibility of nt U37/U38 for cleavage by RNase T2 and of bases A68/G69 for chemical modification suggests that these residues are not stably base paired and part of helix c, but are rather single-stranded and enlarge the internal loop B. In line with this, sequence comparison of bacterial SRP RNA homologues shows the conservation of helix c only up to the U36-G70 base pair (Larsen & Zwieb, 1990).

The most pronounced result of probing with single strand-specific enzymatic and chemical probes is the generally very low reactivity of 4.5S RNA, which indicates an overall compact structure of the RNA and the existence of base pairing interactions across the internal loops of the secondary structure models. Specifically, the lack of modification of C17-G93 and C23-G85 suggests strongly the existence of base pairs in the internal loops E and D, respectively. Also, the data suggest that G49-A60 in the internal loop A are base paired, supporting a proposal by Poritz et al. (1988).

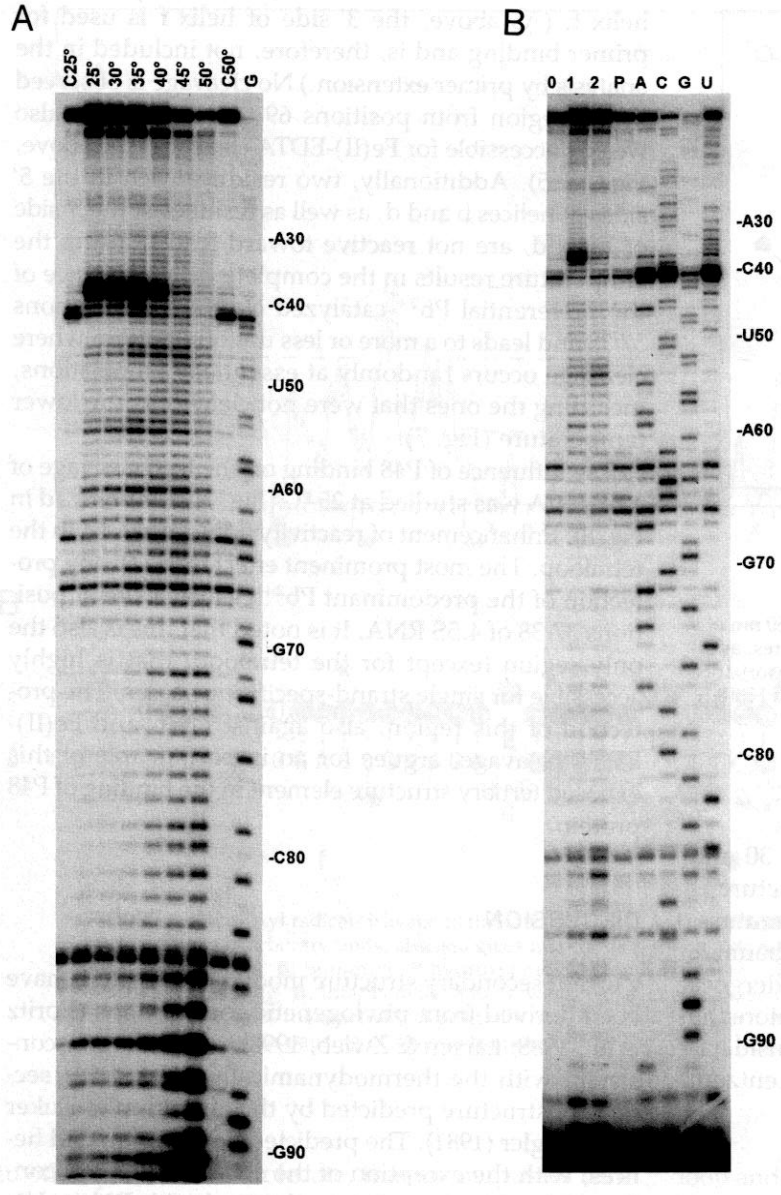

FIGURE 7. Pb^{2+} cleavage of 4.5S RNA. **A:** Temperature dependence of lead-catalyzed cleavage. C25°, control at 25 °C; C50°, control at 50 °C; G, dideoxysequencing, G-lane. **B:** Lead-catalyzed cleavage in the absence and presence of P48 at 25 °C. Lane 0, control incubation of 4.5S RNA alone (20 pmol); lane P, control incubation with 20 pmol P48; lane 1, 4.5S RNA (20 pmol); lane 2, 20 pmol P48 added. A, C, G, U, sequencing lanes.

Guanine residues located in internal loops (G48, G61, G76) that exhibit low or no accessibility for either RNase T1 or kethoxal are probably also involved in interactions not shown in the secondary structure models. The latter two residues may be protected by the tertiary interactions discussed below.

Residues G53, G54, and A55 in the tetraloop show reactivity toward RNases T1 and/or T2, which is even

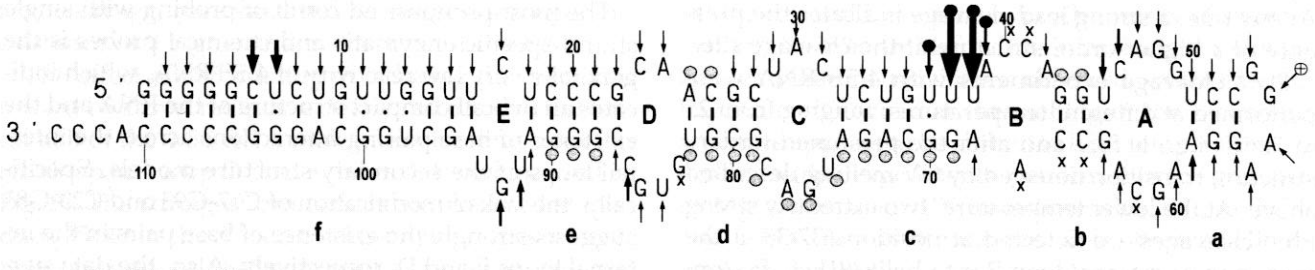

FIGURE 8. Pb^{2+} cleavage pattern of 4.5S RNA. Lead-catalyzed cleavages are indicated by arrows of corresponding thickness. ⊛, positions uncleaved; circles above arrows indicate strong (●) or weak (○) protection or enhancement (⊕) of cleavage by bound P48. x, positions not included in the analysis due to pausing of reverse transcriptase.

enhanced in the presence of P48. Fe(II)-EDTA cleavage of the tetraloop residues is not influenced and lead-catalyzed cleavage at position G54 is enhanced by P48. Thus, it is unlikely that the tetraloop is involved in a tertiary interaction with a double-stranded region of the RNA like the one observed in the class I intron of *Tetrahymena* (Murphy & Cech, 1994).

4.5S RNA is not existing in the rod-like form of the secondary structure model, but rather is folded into a tertiary structure. This was suggested by previous measurements of the rotational behavior of fluorescently labeled 4.5S RNA (Lentzen et al., 1994). The present results support this contention and allow a tentative conclusion as to how the molecule is folded. Most informative in this regard is the asymmetry of the modification patterns obtained with RNases and, in particular, with hydroxyl radicals and with lead ions. They show a general inaccessibility of the apical part of the 3′ side of the molecule extending from the internal loops A–D, whereas the remaining part of the 3′ side as well as the 5′ side of the molecule are more reactive. The data are explained best by a bent structure of 4.5S RNA in which the protected part of the molecule is located inside and the accessible residues outside the structure. In the model depicted in Figure 9, it is assumed that the bending takes place in the highly asymmetric internal loop B, which, as discussed above, is probably larger than shown in the secondary structure models. A complex structure of loop B is consistent with the strong lead cleavage site in the 5′ side of the loop. The disappearance of the lead cleavage site at higher temperature indicates that the tertiary structure and, with that, the Pb^{2+} binding site unfolds upon raising the temperature. Unfolding of a bent tertiary structure of 4.5S RNA is in keeping with the hyperchromicity measurements (Fig. 6) and with data obtained by temperature-gradient gel electrophoresis that show a substantially lower mobility of the unfolded form of the molecule compared to the folded one (Lentzen, 1995).

Binding of protein P48 to 4.5S RNA strongly protects an otherwise exposed region in the apical half of the 5′ side of the RNA, encompassing residues 24–49, and leads to further protection of weakly reactive residues in the corresponding 3′ side, residues 59–84. This is shown by enzymatic as well as chemical probing (Figs. 2, 3). The strong protection of A47 indicates a direct interaction of the base with the protein. The footprint of P48 on 4.5S RNA is delineated most clearly by hydroxyl radical cleavage (Fig. 4). The binding site of P48 is confined to the part of 4.5S RNA that contains all nucleotides conserved among the SRP RNAs, extending from loop A to loop C, and probably somewhat further through the nonconserved helix d into loop D. The site comprises the nucleotides shown to be essential for binding (Wood et al., 1992), of which A39, A47, G48, and G49 are strongly protected by P48. A60 and G61, the two other positions that were also shown to be essential for binding of P48, are not protected against Fe(II)-EDTA cleavage or any other of the applied probes. Thus, we conclude that these residues are not in contact with P48, but rather are necessary for maintaining the structure of the internal loop A; A60 is probably involved in a noncanonical base pairing to G49 (Poritz et al., 1988; Althoff et al., 1994).

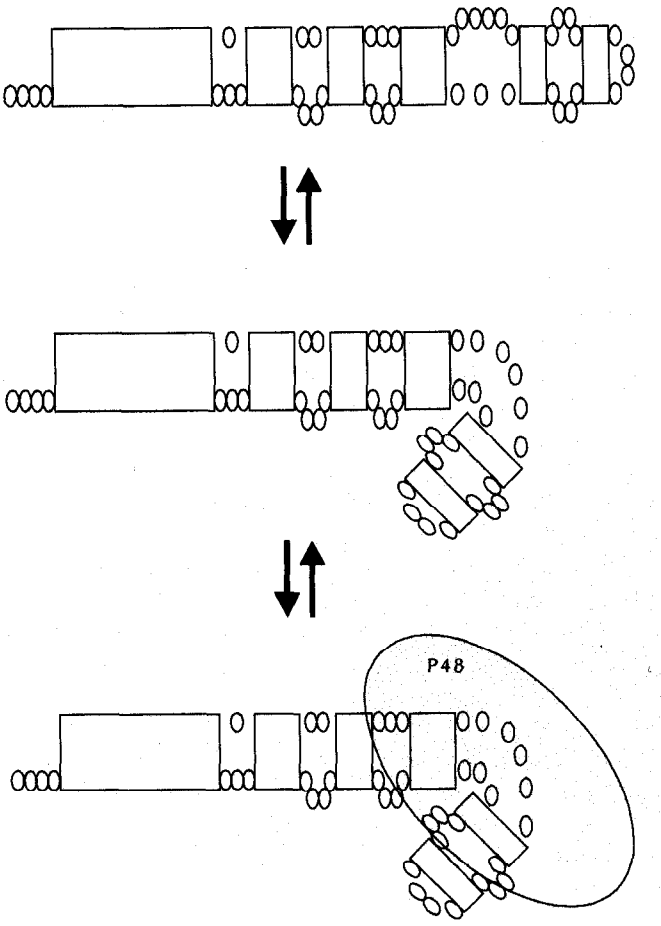

FIGURE 9. Schematic model of the tertiary folding of 4.5S RNA and the P48·4.5S RNA complex. Regions with canonical base pairing are given as rectangles, other nucleotides as circles. For a discussion of the model, see the text.

Not involved in the binding of P48 are the remaining, nonconserved regions of the RNA, helices e and f and the internal loop E. The backbone of the tetraloop also does not interact with P48, as is evident from an enhancement of nuclease cleavage (Fig. 2). The somewhat decreased accessibility for chemical modification of the tetraloop bases in the complex (Fig. 3) may be attributed either to base-specific contacts to P48 not involving the backbone, or to an indirect structural effect. Because exchange of tetraloop bases does not abolish P48 binding (Wood et al., 1992), the latter possibility seems more likely.

In the schematic model depicted in Figure 9, the structure of 4.5S RNA in the complex with P48 is shown as bent. The model is entirely consistent with

all modification results and takes into account that the higher-order structure of 4.5S RNA—interpreted as bent—is prevailing at the conditions of the experiments. Formally, binding of P48 to the unfolded, extended form of the RNA is not excluded by the data. To us, it seems less likely, because it would require the protein to protect both sides of the apical half of 4.5S RNA extending over roughly 5 nm. It should be emphasized, however, that the schematic model of Figure 9 does not imply an unchanged structure of the RNA in the complex. Rather, the structure of 4.5S RNA does change upon formation of the SRP, as evident from the results obtained for the tetraloop, discussed above, and for the 3′ end of the RNA (Lentzen et al., 1994). A transition into a more extended conformation can be achieved in vitro by raising the temperature from 30 °C to 40 °C, as demonstrated by increased cleavage by lead and hydroxyl radicals in the region protected at lower temperature. It is conceivable that this conformational transition has a functional role in vivo. The transition may either correspond to a functional role of the free RNA in a conformation different from the one prevailing in the SRP complex, or to ligand-induced changes of the RNA conformation during the SRP cycle.

MATERIALS AND METHODS

Preparation of 4.5S RNA and P48

4.5S RNA was isolated from overproducing *E. coli* HB101/pSB832 as described (Lentzen et al., 1994) and further purified by 10% polyacrylamide (0.5% bisacrylamide)/8 M urea gel electrophoresis. The RNA was eluted, precipitated twice with ethanol, and resuspended in water. Radioactive labeling at the 3′ end was performed with [5′-^{32}P]pCp and T4 RNA ligase (England & Uhlenbeck, 1978) followed by repurification by denaturing gel electrophoresis. Protein P48 carrying a C-terminal histidine tag was purified by affinity chromatography (Lentzen et al., 1994).

Enzymatic and chemical probing

Samples were preincubated for 15 min at 25 °C in buffer A (20 mM NH_4-HEPES, pH 7.5, 100 mM NH_4Cl, 10.5 mM Mg-acetate, 0.5 mM EDTA). For each reaction, a control was treated in parallel, omitting the reagent. For the enzymatic probing of unlabeled RNA, 20 pmol 4.5S RNA with 0, 20, 40 pmol of P48 were incubated in 9 μL buffer A. Cleavage reactions were started by addition of 1 μL RNase T1 (Sigma, 0.0025 unit), T2 (Sigma, 0.01 unit), or V1 (Pharmacia, 0.005 unit) and incubated for 5 min at 25 °C. The enzymatic cleavages of [^{32}P]4.5S RNA (100.000 cpm = 0.4 pmol) with RNase T1 (0.05 unit), RNase V1 (0.05 unit), and nuclease S1 (50 units, in the presence of 0.1 mM Zn^{2+}) were for 5 min at 25 °C.

DMS modification of 4.5S RNA (15 pmol) was performed in 20 μL of buffer A containing 0.5% or 5% DMS for 5 min at 25 °C. Kethoxal modification of 4.5S RNA (15 pmol) was performed in 20 μL of buffer A containing 15 mg/mL kethoxal for 30 min at 25 °C.

The Fe(II)-EDTA reaction was performed as described (Hüttenhofer & Noller, 1994) in 25 μL of buffer A with 20 pmol of 4.5S RNA, 0–60 pmol P48, 2 mM $(NH_4)_2Fe(SO_4)_2$, 4 mM EDTA, 1 mM DTE, 0.4% H_2O_2. The reaction was incubated for 10 min at 25 °C. All the enzymatic and chemical reactions (except for Fe(II)-EDTA) were stopped by phenol extraction, followed by ethanol precipitation in the presence of 0.3 M sodium acetate and washing with 80% ethanol. The Fe(II)-EDTA reaction was stopped by ethanol precipitation, then phenol-extracted, again precipitated, and washed with 80% ethanol.

Lead cleavage was performed essentially as described (Gornicki et al., 1989). Twenty picomoles of 4.5S RNA with 0–20 pmol of P48 were incubated with 37 mM lead acetate in 15 μL of 80 mM HEPES, pH 7.5, 150 mM potassium acetate, 15 mM magnesium acetate for 5 min at 25 °C. The reaction was terminated by ethanol precipitation in the presence of 33 mM EDTA, phenol extraction, and reprecipitation with ethanol.

Identification of cleavage and modification sites

With end-labeled 4.5S RNA, RNA fragments were sized by electrophoresis on 15% polyacrylamide (0.75% bisacrylamide)/8 M urea slab gels and the cleavage positions were identified by running in parallel RNase T1 and formamide ladders.

For primer extension analysis, two different oligonucleotides, CCCTGCCAGCTA, complementary to nt 94–105 of 4.5S RNA, and GGACCTGACCTGGT, complementary to nt 39–52 of 4.5S RNA, were synthesized with an Applied Biosystems apparatus using the phosphoramidite method. The primers were 5′-labeled with ^{32}P by T4-polynucleotide kinase and purified by 10% polyacrylamide (0.5% bisacrylamide)/8 M urea gel electrophoresis. The cleaved or modified 4.5S RNA was dissolved in water or (for kethoxal modified RNA) in 30 mM sodium borate, pH 7.0. Hybridization of the radioactive primer (80.000 cpm) to the modified or cleaved RNA was performed by incubation for 1 min at 95 °C and 5 min at 25 °C in a total volume of 6 μL. cDNA synthesis was performed in a total volume of 15 μL with 4 units of AMV reverse transcriptase (Life Sciences), 1.5 mM each of the four dNTPs in 50 mM Tris-HCl, 6 mM $MgCl_2$, 40 mM KCl, 12.5% (v/v) DMSO, pH 8.5, for 30 min at 50 °C. Sequencing with chain-terminators was performed in the same way, except that the respective dideoxynucleotide (3.3 μM), the corresponding deoxynucleotide (25 μM), and the other three deoxynucleotides (100 μM) were added. After primer extension, the RNA template was hydrolyzed with KOH (Brunel et al., 1991). Incubation controls were run in parallel in order to detect nicks in the RNA and pauses of reverse transcriptase. The cDNA fragments were then precipitated and analyzed on 8% polyacrylamide (0.4% bisacrylamide)/8 M urea slab gels.

ACKNOWLEDGMENTS

We thank Pascale Romby and Eric Westhof for fruitful discussions and Flore Winter for technical assistance. G.L. was supported by a short-term fellowship of EMBO. The work was supported by Deutsche Forschungsgemeinschaft and the Centre National de la Recherche Scientifique.

Received December 4, 1995; returned for revision January 4, 1996; revised manuscript received January 31, 1996

REFERENCES

Althoff S, Selinger D, Wise JA. 1994. Molecular evolution of SRP cycle components: Functional implications. *Nucleic Acids Res 22*: 1933–1947.

Bernstein HD, Poritz MA, Strub K, Hoben PJ, Brenner S, Walter P. 1989. Model for signal sequence recognition from amino-acid sequence of 54K subunit of signal recognition particle. *Nature 340*: 482–486.

Bernstein HD, Zopf D, Freymann DM, Walter P. 1993. Functional substitution of the signal recognition particle 54-kDa subunit by its *Escherichia coli* homolog. *Proc Natl Acad Sci USA 90*:5229–5233.

Bourgaize DB, Farrell C, Langley KH, Fournier MJ. 1984. Physical properties of the *E. coli* 4.5S RNA: First results suggest a hairpin helix of unusual thermal stability. *Nucleic Acids Res 12*:2019–2034.

Brown S. 1989. Time of action of 4.5S RNA in *E. coli* translation. *J Mol Biol 209*:79–90.

Brunel C, Romby P, Westhof E, Ehresmann C, Ehresmann B. 1991. Three-dimensional model of *Escherichia coli* ribosomal 5 S RNA as deduced from structure probing in solution and computer modeling. *J Mol Biol 221*:293–308.

Connolly T, Gilmore R. 1989. The signal recognition particle receptor mediates the GTP-dependent displacement of signal sequence from the nascent polypeptide. *Cell 57*:599–610.

Dirheimer G, Ebel JP, Bonnet J, Gangloff J, Keith G, Krebs B, Kuntzel B, Roy A, Weissenbach J, Werner C. 1972. Primary structure of transfer RNA. *Biochimie 54*:127–144.

Ehresmann C, Baudin F, Mougel M, Romby P, Ebel J, Ehresmann B. 1987. Probing the structure of RNAs in solution. *Nucleic Acids Res 15*:53–72.

England TE, Uhlenbeck OC. 1978. 3′-terminal labelling of RNA with T4 RNA ligase. *Nature 275*:560–561.

Gilmore R, Blobel G, Walter P. 1982. Protein translocation across the endoplasmic reticulum. I. Detection in the microsomal membrane of a receptor for the signal recognition particle. *J Cell Biol 95*: 463–469.

Gornicki P, Baudin F, Romby P, Wiewiorowski M, Krzyzosiak W, Ebel JP, Ehresmann C, Ehresmann B. 1989. Use of lead(II) to probe the structure of large RNA's. Conformation of the 3′ terminal domain of *E. coli* 16S rRNA and its involvement in building the tRNA binding sites. *J Biomol Struct Dyn 6*:971–984.

Hauser S, Bacher G, Dobberstein B, Lütcke H. 1995. A complex of the signal sequence binding protein and the SRP RNA promotes translocation of nascent proteins. *EMBO J 14*:5485–5493.

Hüttenhofer A, Noller HF. 1994. Footprinting mRNA–ribosome complexes with chemical probes. *EMBO J 13*:3892–3901.

Krzyzosiak WJ, Marciniec T, Wiewiorowski M, Romby P, Ebel JP, Giege R. 1988. Characterization of the lead(II)-induced cleavages in tRNAs in solution and effect of the y-base removal in yeast $tRNA^{Phe}$. *Biochemistry* 27:5771–5777.

Kusters R, Lentzen G, Eppens E, Vangeel A, Vanderweijden CC, Wintermeyer W, Luirink J. 1995. The functioning of the SRP receptor FtsY in protein-targeting in *E. coli* correlated with its ability to bind and hydrolyse GTP. *FEBS Lett 372*:253–258.

Larsen N, Zwieb C. 1990. SRP-RNA sequence alignment and secondary structure. *Nucleic Acids Res 19*:209–215.

Latham JA, Cech TR. 1989. Defining the inside and outside of a catalytic RNA molecule. *Science 245*:276–282.

Lentzen G. 1995. Structure and function of the signal recognition particle (SRP) of *Escherichia coli*. PhD thesis, University Witten/ Herdecke.

Lentzen G, Dobberstein B, Wintermeyer W. 1994. Formation of SRP-like particle induces a conformational change in *E. coli* 4.5S RNA. *FEBS Lett 348*:233–238.

Luirink J, High S, Wood H, Giner A, Tollervey D, Dobberstein B. 1992. Signal-sequence recognition by an *Escherichia coli* ribonucleoprotein complex. *Nature 359*:741–743.

Luirink J, Tenhagenjongman CM, Vanderweijden CC, Oudega B, High S, Dobberstein B, Kusters R. 1994. An alternative protein targeting pathway in *Escherichia coli*: Studies on the role of FtsY. *EMBO J 13*:2289–2296.

Lütcke H. 1995. Signal recognition particle (SRP), a ubiquitous initiator of protein translocation. *Eur J Biochem 228*:531–550.

Meyer DI, Krause E, Dobberstein B. 1982. Secretory protein translocation across membranes—The role of the "docking protein." *Nature 297*:647–650.

Miller JD, Bernstein HD, Walter P. 1994. Interaction of *E. coli* Ffh/4.5S ribonucleoprotein and FtsY mimics that of mammalian signal recognition particle and its receptor. *Nature 367*:657–659.

Murphy FL, Cech TR. 1994. GAAA tetraloop and conserved bulge stabilize tertiary structure of a group I intron domain. *J Mol Biol 236*:49–63.

Pan T, Gutell RR, Uhlenbeck OC. 1991. Folding of circularly permuted transfer RNAs. *Science 254*:1361–1364.

Phillips GJ, Silhavy TJ. 1992. The *E. coli* ffh gene is necessary for viability and efficient protein export. *Nature 359*:744–746.

Poritz MA, Bernstein HD, Strub K, Zopf D, Wilhelm H, Walter P. 1990. An *E. coli* ribonucleoprotein containing 4.5S RNA resembles mammalian signal recognition particle. *Science 250*:1111–1117.

Poritz MA, Strub K, Walter P. 1988. Human SRP RNA and *E. coli* 4.5S RNA contain a highly homologous structural domain. *Cell 55*:4–6.

Ribes V, Römisch K, Giner A, Dobberstein B, Tollervey D. 1990. *E. coli* 4.5S RNA is part of a ribonucleoprotein particle that has properties related to signal recognition particle. *Cell 63*:591–600.

Römisch K, Webb J, Herz J, Prehn S, Frank R, Vingron M, Dobberstein B. 1989. Homology of 54K protein of signal-recognition particle, docking protein and two *E. coli* proteins with putative GTP-binding domains. *Nature 340*:478–482.

Rosenbaum V, Riesner D. 1987. Temperature-gradient gel electrophoresis: Thermodynamic analysis of nucleic acids and proteins in purified form and in cellular extracts. *Biophys Chem 26*:235–246.

Samuelsson T. 1992. A mycoplasma protein homologous to mammalian SRP54 recognizes a highly conserved domain of SRP RNA. *Nucleic Acids Res 20*:5763–5770.

Siegel V, Walter P. 1988. The affinity of signal recognition particle for presecretory proteins is dependent on nascent chain length. *EMBO J 7*:1769–1775.

Tullius TD. 1987. Chemical "snapshots" of DNA: Using the hydroxyl radical to study the structure of DNA and DNA-protein complexes. *Trends Biochem Sci 12*:297–300.

Walter P, Blobel G. 1982. Signal recognition particle contains a 7S RNA essential for protein translocation across the endoplasmic reticulum. *Nature 299*:691–698.

Walter P, Ibrahimi I, Blobel G. 1981. Translocation of proteins across the endoplasmic reticulum. I. Signal recognition protein (SRP) binds to in-vitro-assembled polysomes synthesizing secretory protein. *J Cell Biol 91*:545–550.

Walter P, Johnson AE. 1994. Signal sequence recognition and protein targeting to the endoplasmic reticulum membrane. *Annu Rev Cell Biol 10*:87–119.

Wood H, Luirink J, Tollervey D. 1992. Evolutionary conserved nucleotides within the *E. coli* 4.5S RNA are required for association with P48 in vitro and for optimal function in vivo. *Nucleic Acids Res 20*:5919–5925.

Wu JC, Kozarich JW, Stubbe J. 1983. The mechanism of free base formation from DNA by bleomycin. A proposal based on site specific tritium release from poly(dA·dU). *J Biol Chem 258*:4694–4697.

Zuker M, Stiegler P. 1981. Optimal computer folding of large RNA sequences using thermodynamics and auxiliary information. *Nucleic Acids Res 9*:133–148.

Zwieb C, Larsen N. 1994. The signal recognition particle database (SRPDB). *Nucleic Acids Res 22*:3483–3484.